Time-resolved infrared spectroscopic study of the switching dynamics of a surface-stabilized ferroelectric liquid crystal

J. G. Zhao,[1] T. Yoshihara,[2] H. W. Siesler,[3] and Y. Ozaki[1,*]
[1]*Department of Chemistry, School of Science, Kwansei-Gakuin University, 2-1 Gakuen, Sanda, Hyogo 669-1337, Japan*
[2]*Display Laboratories, Fujitsu Laboratories Limited, Ohkubo, Akashi 674-0054, Japan*
[3]*Department of Physical Chemistry, University of Essen, D-45117 Essen, Germany*
(Received 27 July 2001; published 25 January 2002)

The orientation dynamics of a ferroelectric liquid crystal with a naphthalene ring (FLC-3) during the electric-field-induced switching between two surface-stabilized states was investigated by means of time-resolved Fourier-transform infrared spectroscopy. Time-resolved infrared spectra of the planar-aligned cell of FLC-3 were measured as a function of the polarization angle ranging from 0° to 180° under a rectangular electric field ±40 V with a 5-kHz repetition rate in the smectic-*C** (Sm-*C**) phase at 137 °C. From these spectra details about the mutual arrangement of different molecular segments at all the delay times in the Sm-*C** phase were derived. It was found that the C═O group in the core moiety exhibits a dynamical behavior different from that in the chiral moiety during the electric-field-induced switching between the two surface-stabilized states. The most important finding in the present study is that during the electric-field-induced switching the FLC molecule not only rotates around the layer normal, but also revolves around its own long axis. Furthermore, time-resolved infrared spectroscopy revealed that each group in the core moiety passes almost simultaneously through the projection of the layer normal in the cell window during the dynamic switching.

DOI: 10.1103/PhysRevE.65.021710 PACS number(s): 61.30.Eb

INTRODUCTION

The basic geometry of a surface-stabilized ferroelectric liquid crystal (FLC) molecule can be described by a director *n* (local average of the molecular axis) that may be identified with the optical axis (we disregard the small biaxiality) and is tilted at a certain angle away from the layer normal of the FLC [1–5]. The only freedom of motion is, therefore, described by the azimuthal variable defined in a plane perpendicular to the layer normal. In recent years, infrared polarization spectroscopy and time-resolved infrared spectroscopy have proven powerful tools for the investigation of the statistical orientational conformation and the dynamical behavior of FLC molecules [6–34]. Measurements of the polarization angle dependence for the intensities of selected infrared bands are very useful to explore the molecular structure and alignment of FLC molecules in the smectic-*C** (Sm-*C**) phase. In a previous study we have proposed a new theory for analyzing the polarization angle dependence of FLC molecules in the surface-stabilized ferroelectric liquid crystal (SSFLC) states [35]. The theory describes the relationship between the intensity of selected absorption bands and the polarization angle of the infrared radiation.

Time-resolved vibrational spectroscopy, especially time-resolved infrared absorption, has been of particular usefulness for investigating the orientational and conformational changes during the electric-field-induced dynamical switching of FLC in the Sm-*C** phase. Several time-resolved infrared studies indicated that during the electric-field-induced dynamical switching, the molecules reorient as rigid units and all the molecular segments reorient nearly simultaneously whereas other studies showed that the different molecular segments have different response and reorientation times [20–31]. Our previous dynamic polarized infrared absorption study has revealed that the core responds instantaneously on switching the electric field, while the chiral and achiral alkyl chains require an induction period before responding to the electric field [29]. In spite of intensive time-resolved infrared studies on the switching dynamics of FLCs at a molecular segmental level, many basic aspects of the dynamical behavior of FLCs have not yet been clarified.

The purpose of the present study is to explore the molecular dynamical orientation of the FLC with a naphthalene ring (FLC-3; Fig. 1) during the electric-field-induced dynamical switching by measuring temporal absorption responses of selected infrared bands over a continuous range of polarizer orientation. The experiments are divided into two parts; the polarization angle dependence of selected bands at various delay times and the time-dependent measurements of their absorption intensity. By the former experiment the projection of the molecular long axis in a cell window can be determined for the delay times via the spatial evolution of the polarization direction with an interval of 5°. Using the latter experiment the dynamics of the projection of the molecular long axis, i.e., the polarization angle corresponding to the

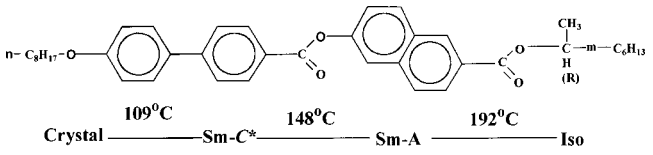

FIG. 1. Structure of FLC-3 and the phase transition temperature.

*Author to whom correspondence should be addressed. FAX: +81-795-65-9077; email address: ozaki@kwansei.ac.ip

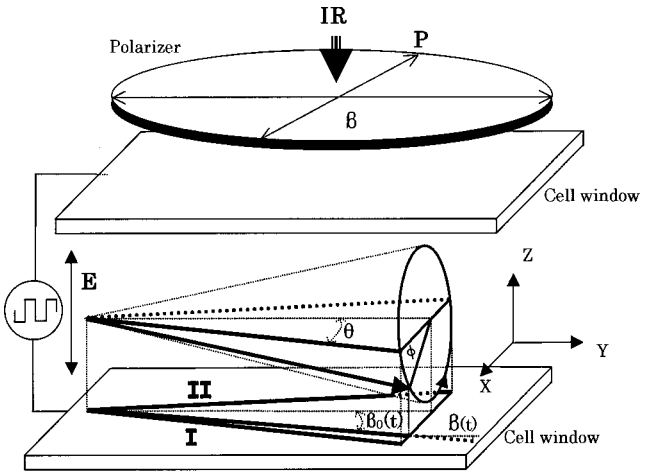

FIG. 2. Schematic arrangement for the time-resolved infrared measurements. I and II are the projections of the directions of the molecular long axis in the plane of the cell window for surface-stabilized states of the ferroelectric liquid crystal, $\phi=\phi(t)$, $\phi(t)$ is the director rotation azimuth angle of the director around the cone at a delay time, θ is the cone angle, $\beta_0(t)$ is the angle between the projection of the molecular long axis and the projection of layer normal in the plane of the cell window, $\beta(t)$ is the angle between the projection of the molecular long axis and the projection of the horizontal polarization of the incidence infrared light in the plane of the cell window, P is the polarization direction of an arbitrary polarizer setting making an angle β with the horizontal polarization of the incidence infrared light, Z parallel to the propagation direction of the incident infrared radiation, X and Y represent the horizontal and vertical polarizations of the propagation direction of the incident infrared radiation, and E is the direction of the applied electric field.

maximum and the minimum absorbances can be observed with the delay time. By selecting specific vibrational modes, particularly for the core and the carbonyl groups, the time evolution of the selected bands can be analyzed. By changing the polarity of the external applied electric field, the permanent electric dipole will rotate by 180° to point in the opposite direction. As a result, the molecular long axis can switch between the two SSFLC states. However, the dynamical behavior of an FLC molecule itself has never been investigated in more detail. The results of the present study clearly reveal the dynamical behavior of molecular reorientation during the electric-field-induced dynamical switching. It has been found that the molecules not only rotate around the layer normal but also revolve around its own long axis.

The present results also show that the maximum and minimum absorbance changes for selected infrared bands are dependent on the polarization angle during the electric-field-induced dynamical switching. Moreover, the polarization angles corresponding to the maximum- and minimum-absorbance variations shift to smaller values as the delay time increases.

EXPERIMENTS

The sample was synthesized and characterized according to the reported procedure [36]. The structure and phase transition sequence of the liquid crystal molecule are shown in Fig. 1. The sample cell consisted of two BaF_2 plates coated with conducting layers of indium tin oxide and polyimide rubbed in one direction. The thickness between the two plates was adjusted by a silicon spacer and has been determined to be 1.7 μm from the interference fringe pattern. The cell was filled with the molten sample by capillary action, heated to the isotropic phase, and then slowly cooled down to a temperature in the Sm-C^* phase. Cyclic temperature treatment was employed to obtain a good homogeneous alignment. Temperature was controlled to an accuracy of ± 0.05 °C with the aid of a METTLER FP80HT thermocontroller. The approximate size of the domains was in the range of several hundred micrometers.

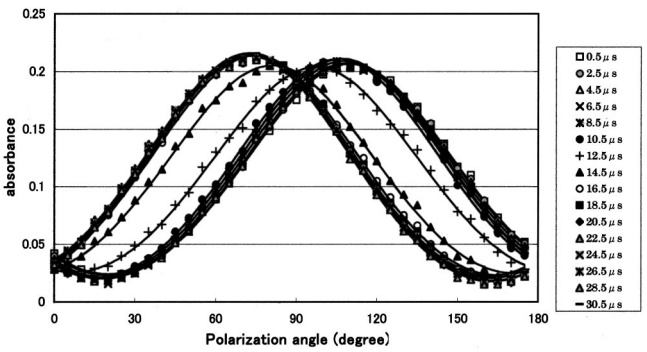

FIG. 3. Peak absorbance versus the polarization angle for the band at 1602 cm^{-1} due to the ring stretching mode of the benzene and naphthalene rings during the dynamical switching of FLC-3 in the Sm-C^* phase at 137 °C at a rectangular electric field of ± 40 V with 5-kHz repetition rate for the delay time from 0.5 to 30.5 μs at an interval of 2 μs.

The time-resolved infrared measurements were made by use of a multichannel asynchronous time-resolving Fourier-transform infrared (FT-IR) system. The details of this novel system were described in Refs. [37,38]. A wire grid polarizer was rotated about the propagation direction of the infrared radiation at an interval of 5°. A rectangular electric field of ± 40 V and 5-KHz repetition rate was applied to the electrodes of the cell from a function generator (SONY AFG310). The gate of the multichannel system was opened every 2 μs in the time range from 0.5 to 30.5 μs. Thus, the time-resolved spectra were measured from 0.5 to 30.5 μs at an interval of 2 μs with a spectral resolution of 4 cm^{-1}. In order to obtain the polarization direction of the maximum absorbance, the polarization angle is varied from 0° to 180° at an interval of 5°. The measurement geometry is illustrated in Fig. 2. The absorbance versus the time and polarization angle can be described as follows:

$$A_{t-p}=-S\log_{10}\{T_{\mathrm{per}}(t)\sin^2[\beta-\beta(t)]+T_{\mathrm{par}}(t)\cos^2 \times[\beta-\beta(t)]\}+A_{\mathrm{iso}}(1-S) \quad (1)$$

where T_{par} and T_{per} are the transmittances of the incident radiation whose polarization directions are parallel and perpendicular to the projection direction of the molecular long axis in the cell window, respectively. $S \geqslant 0$ is a constant, which represents the contribution of a perfectly uniaxial

TABLE I. $\beta(t)$ of representative infrared bands during the dynamical switching of FLC-3 in the Sm-C^* phase at 137 °C at a rectangular electric field of ±40 V with 5-kHz repetition rate for the delay time from 0.5 to 30.5 μs at an interval of 2 μs.

Bands (cm^{-1}) Delay time (μs)	1066	1095	1146	1188	1262	1273	1473	1496	1524	1602	1715	1736
0.5	110.09	103.26	108.46	108.1	108.16	107.77	108.8	110	113.02	109.93	97.14	95.48
2.5	109.58	103.27	108.31	107.56	107.82	107.48	109.12	109.89	112.53	109.75	97.4	96.09
4.5	108.8	103.27	107.66	106.84	107.28	106.7	107.75	109.02	111.38	108.98	97.36	96.1
6.5	107.8	102.01	106.9	106	106.27	105.89	106.59	108.35	110.16	107.78	97.38	96.17
8.5	107.09	101.51	105.91	105.22	105.7	105.13	106.07	107.5	109.02	106.88	96.6	95.21
10.5	105.27	100.65	104.54	103.92	104.16	103.76	101.05	105.62	108.77	105.36	96.29	95.62
12.5	97.15	95.05	96.89	96.81	96.83	96.62	97.21	97.45	98.32	97.21	92.85	93.12
14.5	80.99	84.72	81.78	82.46	82.06	82.12	87.7	80.03	79.13	80.91	86.8	88.9
16.5	74.58	80.14	76.17	76.87	76.54	76.79	76.48	74.24	72.44	74.61	83.93	87.25
18.5	73.37	79.1	74.57	75.58	75.05	75.42	75.28	73.1	71.6	73.37	82.81	86.53
20.5	72.92	79.03	74.26	75.08	74.71	74.93	74.44	72.34	71.75	73.11	82.94	86.58
22.5	72.63	78.84	74.03	74.87	74.36	74.74	74.23	72.11	72.05	72.63	83.52	87.03
24.5	72.56	78.83	74.06	74.75	74.44	74.65	73.69	72.09	70.92	72.56	82.21	87.2
26.5	72.46	78.47	73.64	74.66	74.35	74.65	73.96	72.69	71.63	72.49	83.08	86.68
28.5	72.31	78.37	73.8	74.64	74.26	74.54	73.56	71.87	70.65	72.71	82.89	86.57
30.5	72.75	77.96	73.6	74.64	71.13	74.47	73.49	71.84	70.08	72.35	83.01	86.44

phase to A_{t-p}. Therefore, we can apply curve fitting using Eq. (1) by a least squares method to obtain the polarization direction of the maximum absorbance [35].

DISCUSSION AND RESULTS

To investigate the segmental dynamics of the FLC, time-resolved FT-IR spectra were measured for a series of polarization angles. These spectra were measured in the 1800–1000 cm^{-1} region over a delay time range from 0.5 to 30.5 μs at an interval of 2 μs and for the polarization angles from 0° to 180° at an interval of 5°. From these spectra one can obtain the information about the molecular orientation in the spatial dimension by analyzing the polarization angle dependence of the absorbance. Furthermore, by analyzing the time dependence of the absorption maximum, one can reach the information concerning the molecular reorientation in the time dimension. To characterize the reorientation of the molecular segments, several representative bands are chosen, including the bands at 1736 (C═O stretching in the core moiety), 1715 (C═O stretching in the chiral moiety), 1602 (C═C ring stretching), 1524 (C═C ring stretching), 1496 (C═C ring stretching), 1473 (CH_2 scissoring), 1273 (C—O—C), 1262 (C—O—C), 1188 (C—O—C), 1146 (C—O—C), 1095 (C—O—C in the chiral moiety), and 1066 cm^{-1} (C—O—C). The band assignments of these bands were reported in Ref. [35].

The plot of the absorbance for the band at 1602 cm^{-1} versus the polarization angle β at all the delay times is presented in Fig. 3. Each symbol represents the measurement data, and the lines represent the results of the curve fitting. The details of the curve fitting were described in Ref. [35]. The angle $\beta(t)$, which corresponds to the absorption maximum in the polarization angles, means the orientation pro-

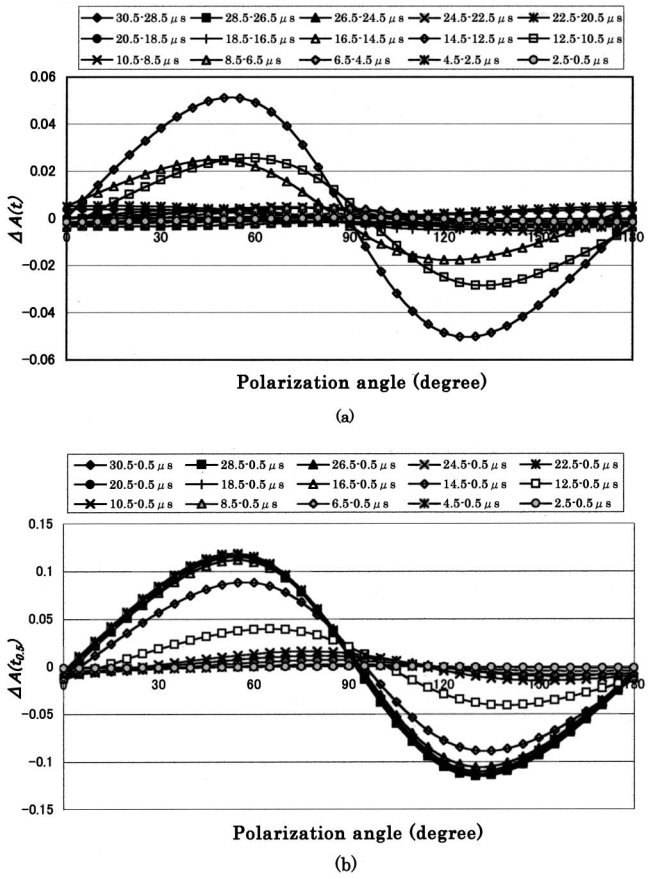

FIG. 4. (a) $\Delta A(t)$ and (b) $\Delta A(t_{0.6})$ versus polarization angle for the band at 1602 cm^{-1} during the dynamical switching of FLC -3 in the Sm-C^* phase at 137 °C at a rectangular electric field of ±40 V with 5-kHz repetition rate for the delay time from 0.5 to 30.5 μs at an interval of 2 μs.

jection direction of the molecular long axis in the cell window. $\beta(t)$ is obtained for all the delay times and shown in Table I. In the same way, $\beta(t)$ obtained for other selected bands is also shown in Table I. Figure 3 reveals that the changes of the polarization angle for the maximum and minimum absorbances are very small for most of the delay times, but they are significant for the delay times of 12.5 and 14.5 μs. From Table I, we see that the polarization angles of 97.21° and 80.91° give the maximum absorbance at the delay times of 12.5 and 14.5 μs, respectively. These two angles are far from $\beta(t)$ of the two surface-stabilized FLC states. In this case, it can be seen from Fig. 2 that the orientation of the FLC molecules at the delay times of 12.5 and 14.5 μs makes a larger inclination than that at other delay times with respect to the plane of the cell window. Consequently, the maximum- and minimum-absorbance changes for the delay times at 12.5 and 14.5 μs are different from those for other delay times. These experimental results suggest that the molecules of the FLC rotate on the orbit of the cone.

Figures 4(a) and 4(b) plot the absorbance change versus polarization angle β for the band at 1602 cm^{-1} at all the delay times. In Figs. 4(a) and 4(b) the absorbance changes between the current and the last delay time $[\Delta A(t)]$ and the absorbance changes between the current and the delay time of 0.5 μs $[\Delta A(t_{0.5})]$ are shown, respectively, for the delay times at 2.5, 4.5,...,28.5, 30.5 μs. $\Delta A(t)$ and $\Delta A(t_{0.5})$ can be expressed as follows:

$$\Delta A(t) = -S \ln \times \frac{A_{\mathrm{per}} \sin^2[\beta-\beta(t)] + A_{\mathrm{par}} \cos^2[\beta-\beta(t)]}{A_{\mathrm{per}} \sin^2[\beta-\beta(t-2)] + A_{\mathrm{per}} \cos^2[\beta-\beta(t-2)]} \tag{2}$$

TABLE II. $\beta(t-2)_{\max}$, $\beta(t-2)_{\min}$, $\beta(t_{0.5})_{\max}$ and $\beta(t_{0.5})_{\min}$ for the band at 1602 cm^{-1} during the dynamical switching of FLC-3 in the Sm-C^* phase at 137 °C at a rectangular electric field of ±40 V with 5-kHz repetition rate for the delay time from 0.5 to 30.5 μs at an interval of 2 μs.

$t-2$ (μs)	$\beta(t-2)_{\max}$ (deg)	$\beta(t-2)_{\min}$ (deg)	$t_{0.5}$ (μs)	$\beta(t_{0.5})_{\max}$ (deg)	$\beta(t_{0.5})_{\min}$ (deg)
2.5–0.5	95	173	2.5-0.5	95	174
4.5–2.5	84	160	4.5-0.5	87	163
8.5–4.5	80	155	6.5-0.5	83	159
8.5–6.5	73	147	8.5-0.5	81	156
10.5–8.5	69	142	10.5-0.5	77	151
12.5–10.5	58	132	12.5-0.5	65	140
14.5–12.5	52	127	14.5-0.5	57	133
16.5–14.5	47	173	16.5-0.5	55	132
18.5–16.5	46	120	18.5-0.5	54	131
20.5–18.5	59	139	20.5-0.5	54	131
22.5–20.5	91	140	22.5-0.5	54	131
24.5–22.5	63	146	24.5-0.5	54	131
26.5–24.5	53	130	26.5-0.5	54	131
28.5–26.5	92	16	28.5-0.5	54	131
30.5–28.5	90	12.5	30.5-0.5	54	131

$$\Delta A(t_{0.5}) = -S \ln \frac{A_{\mathrm{per}} \sin^2[\beta-\beta(t)] + A_{\mathrm{par}} \cos^2[\beta-\beta(t)]}{A_{\mathrm{per}} \sin^2[\beta-\beta(t_{0.5})] + A_{\mathrm{par}} \cos^2[\beta-\beta(t_{0.5})]}, \tag{3}$$

where $\beta(t_{0.5})$ is $\beta(t)$ at the initial delay time. When $\partial \Delta A(t_{0.5})/\partial\ \beta = 0$ and $\partial \Delta A(t)/\partial\ \beta = 0$, the maximum and minimum of $\Delta A(t)$ and $\Delta A(t_{0.5})$ corresponding to the polarization angle $\beta(t-2)_{\max}$, $\beta(t-2)_{\min}$, $\beta(t_{0.5})_{\max}$, and $\beta(t_{0.5})_{\min}$ can be calculated for the band at 1602 cm^{-1} (see Table II). It is noted that at each delay time, the curves of both $\Delta A(t)$ and $\Delta A(t_{0.5})$ versus the polarization angle have a maximum and minimum and that the corresponding polarization angles shift to smaller values with the increase in the delay time. The decrease in the polarization angles giving the maximum and the minimum may be ascribed to the switching motion of the FLC molecules on the tilt cone. Due to the presence of this shift, it is necessary to select an appropriate polarization angle in order to analyze precisely the reorientation of the segments as a function of the delay time.

To analyze the changes in the direction of the molecular long axis with the delay time, $\beta_0(t)$ for the representative bands was calculated and shown in Fig. 5. One can observe that $\beta_0(t)$ is very similar for the bands at 1602, 1524, 1496, 1273, 1262, 1188, 1146, and 1066 cm^{-1} at different delay times. This reveals that the core moiety of the FLC molecule retains a rod-shaped conformation during the electric-field-induced switching. $\beta_0(t)$ of the bands at 1736 and 1715 cm^{-1} exhibits a large deviation from those of other bands, e.g., the bands at 1602 and 1188 cm^{-1}. This is due to the hindered rotation of the C═O groups. $\beta_0(t)$ of the band at 1095 cm^{-1} also deviates from those of the other bands, suggesting that for the C—O—C linkage in the chiral moiety, the intermolecular interaction is weaker than in the core moiety. Moreover, it can be seen from Fig. 5 that $\beta_0(t)$ for all selected bands switches symmetrically from a positive angle to a negative angle. Figure 5 also elucidates that the motional

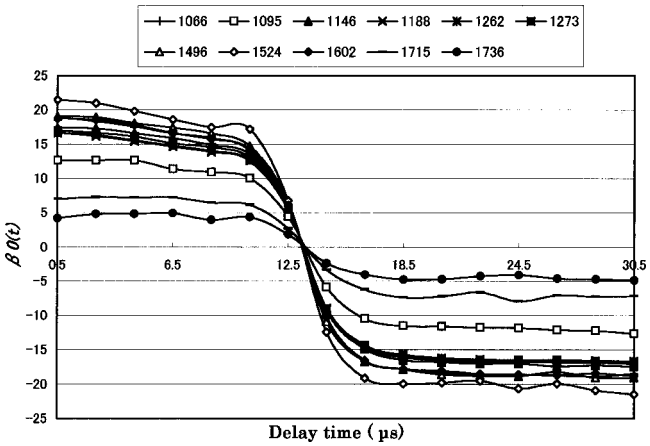

FIG. 5. $\beta_0(t)$ vs delay time for representative infrared bands of FLC-3 in the Sm-C^* phase at 137 °C at a rectangular electric field of ±40 V with 5-kHz repetition rate for the delay time from 0.5 to 30.5 μs at an interval of 2 μs.

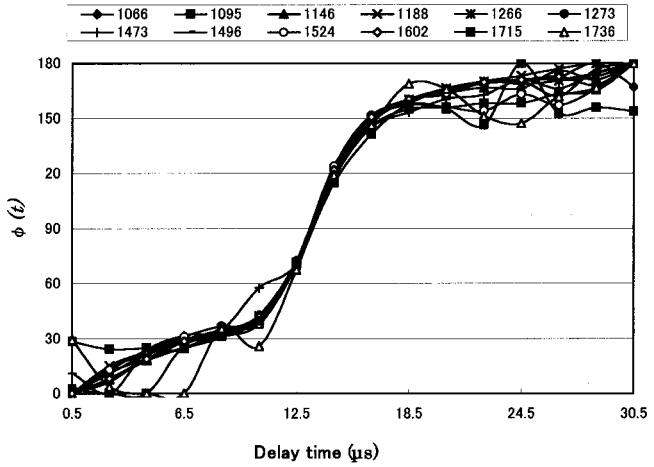

FIG. 6. $\phi(t)$ versus delay time for representative infrared bands of FLC-3 in the Sm-C^* phase at 137 °C at a rectangular electric field of ± 40 V with 5-kHz repetition rate for the delay time from 0.5 to 30.5 μs at an interval of 2 μs.

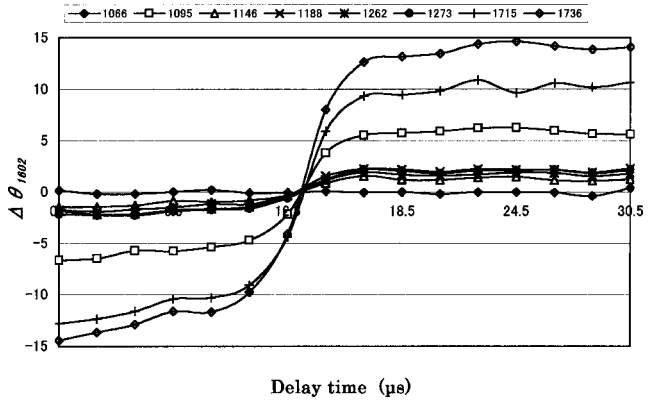

FIG. 7. Time dependence of $\Delta\theta_{1602}$ versus delay time for some representative infrared bands of FLC-3 in the Sm-C^* phase at 137 °C at a rectangular electric field of ±40 V with 5-kHz repetition rate for the delay time from 0.5 to 30.5 μs at an interval of 2 μs.

behavior of the projection direction in the cell window of the orientation of representative bands is different at most delay times.

So far it has been a very difficult problem to directly observe the rotation around the orbit of the cone of an FLC molecule by infrared spectroscopy. In Fig. 2, the relationship between $\beta_0(t)$ and the azimuthal angle $\phi(t)$ is given. It can be written as follows:

$$\phi(t)=\cos^{-1}\left(\frac{\tan\beta_0(t)}{\tan\theta}\right), \tag{4}$$

where $-\theta\leqslant\beta_0(t)\leqslant\theta$. Therefore, it can be inferred that $0\leqslant\phi(t)\leqslant\pi$. $\phi(t)$ for the representative bands calculated by Eq. (4) are shown in Fig. 6. Here, we assume that delay times of 0.5 and 30.5 μs correspond to $-\theta$ and θ, respectively. From Fig. 6, it can be seen that all the selected bands almost pass through $\phi(t)=90°$ at the same time.

We have analyzed the dynamic behavior of the projection direction of the molecular long axis relative to the polarization direction of the incident radiation. The results reveal that the molecular long axis rotates around the conical orbit during the electric-field-induced switching. Previous time-resolved infrared studies mainly considered the motion of an FLC molecule by using a coordinate system based on the polarization direction of the polarizer [14,18,27–29,31–33]. Therefore, the studies could not be used to analyze the relative motion of different segments in the molecules. The orientation of the band at 1602 cm^{-1} is selected as a reference coordinate system, and the orientation of other representative bands referring to it makes an angle $\Delta\theta_{1602}$. The plot of $\Delta\theta_{1602}$ versus the delay time during the course of switching is shown in Fig. 7. $\Delta\theta_{1602}$ of the selected bands varies with the delay time and increases from negative angles to positive ones, indicating the changes in the orientation for selected bands with reference to the band at 1602 cm^{-1} during the electric-field-induced switching. These changes may be caused by the revolution of the molecule around its own axis induced by the electric torque $\Gamma=\mathbf{P}\times\mathbf{E}$, where $\mathbf{P}$ is the total polarization of the FLC [5]. Therefore, it seems that the electric torque Γ plays two roles: (1) to make the molecule revolve around its own axis and (2) to make the molecule rotate around the tilt cone. From Fig. 7, it is found that the C═O group in the core moiety shows a different dynamic behavior compared to that in the chiral moiety during the electric-field-induced switching between the two surface-stabilized states. The orientation of the former C═O groups is symmetrical to the orientation of the band at 1602 cm^{-1}, but the orientation of the latter is asymmetrical. This indicates that dynamical behavior of the C═O group in the core moiety may be more free than the C═O group in the chiral moiety during the course the molecule revolves around its own axis in the electric-induced switching.

The relationship between $\phi(t)$ and the delay time has been described above. One can define the average angular velocity of the FLC molecule rotating around the layer normal as $\omega=\Delta\phi/\Delta t$, where in this paper $\Delta\phi=\phi(t+2)-\phi(t)$, $\Delta t=2\,\mu$s, and the average angular velocity $\omega=\omega(t+1)$. Figure 8 shows the plot of ω versus the delay time during the course of switching for the selected bands at 1602, 1273, 1262, 1188, 1146, and 1066 cm^{-1}. This plot clearly indicates that the average angular velocity of various bands is different within several microseconds of the initial and final delay time. Many reports claimed that different molecular segments do not reorient simultaneously during the electric-field-induced switching [28,29,31]. This different response of molecular segments is the cause for the fact that the average angular velocity reflected by various bands is different during the initial microseconds of the delay time. Each molecule of an FLC is subjected to three types of main torques [39]: the viscous torque, which is proportional to the angular velocity of the molecular director on the tilt cone and rotational viscosities of the medium, the electric torque and the elastic torque. In the accelerating course of the initial microseconds, the viscous torque is very small. The electric torque is also very small. Owing to the unbalanced influence of the torques, different molecular segments have a different

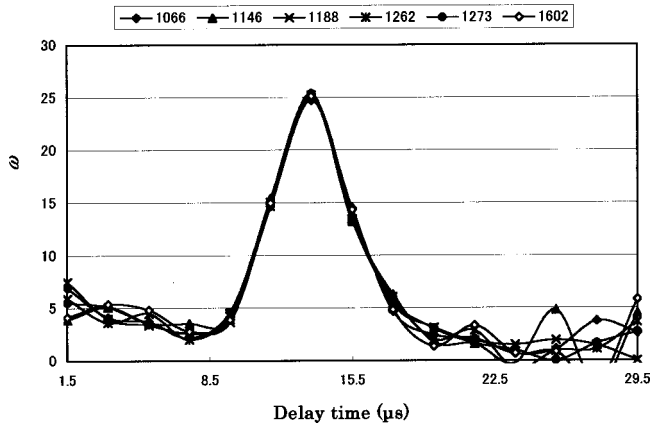

FIG. 8. A average angle velocity ω versus delay time for some representative infrared bands of FLC-3 in the Sm-C^* phase at 137 °C at a rectangular electric field of ± 40 V with 5-kHz repetition rate.

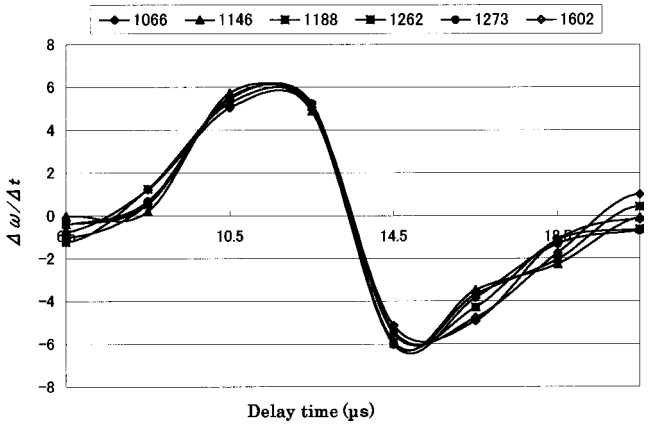

FIG. 9. Average angular acceleration $\Delta\omega/\Delta t$ versus delay time for some representative infrared bands of FLC-3 in the Sm-C^* phase at 137 °C at a rectangular electric field of ± 40 V with 5-kHz repetition rate.

behavior of motion. During the retardation of the final microseconds, the direction of the electric torque is opposite to the corresponding accelerated course on the tilt cone, but the magnitude of the electric torque and its change are equal for the two courses. Therefore, the motion behavior in the latter course is similar to that in the former. When the molecules tend to $\phi(t)=90°$; all torques are also towards equilibrium, and the angular velocity of all segments simultaneously tends to reach their maximum angular velocity. This means that all the torques reach a balanced position.

To explore the response of different molecular segments to the applied rectangular electric field in more detail, we have plotted the angular acceleration of the representative bands at different time delays in Fig. 9. From this figure we clearly find the positive and negative angular accelerations during the electric-field-induced switching. The cause of this accelerating course is that the ferroelectric and the dielectric torques are functions of the azimuthal angle ψ between the spontaneous polarization and the electric field. As a result, the electric torque is also a function of the delay time under the applied rectangular electric field, changing from a positive torque to a negative one. The results reveal that the ferroelectric case is completely different from the nematic case in which the electric torque changes undirectionally.

CONCLUSIONS

The present study using time-resolved infrared spectroscopy has demonstrated that the FLC molecule not only rotates around the layer normal, but also revolves around its own long axis. It has also clearly shown that the orientation of structural segments in the core moiety passes almost simultaneously through the projection of the normal of the layer in the cell window during the dynamic switching. These results have revealed that the maximum- and minimum-absorbance changes for selected infrared bands are dependent on the polarization angle during the electric-field-induced dynamical switching. Moreover, the maximum- and minimum-associated polarization angles shift to smaller values as the delay time increases. It has been also found that the C═O group in the core moiety exhibits a dynamical behavior different from that in the chiral moiety during the electric-field-induced switching between the two surface-stabilized states. The orientation of the C═O groups in the core is symmetrical to the orientation of the band at 1602 cm^{-1}, but the orientation of the C═O group in the chiral moiety is not symmetrical. This indicates that the dynamical behavior of the C═O group in the core moiety is more free than the C═O group in the chiral moiety during the course of the revolution around its own axis in the electric-induced switching.

[1] N. A. Clark and S. T. Lagerwall, Appl. Phys. Lett. **36**, 899 (1980).
[2] N. A. Clark and S. T. Lagerwall, Ferroelectrics **59**, 25 (1984).
[3] S. T. Lagerwall, N. A. Clark, J. Dijon, and J. F. Clerc, Ferroelectrics **94**, 3 (1989).
[4] J. S. Patel and J. W. Goodby, Opt. Eng. **26**, 373 (1987).
[5] S. T. Lagerwall, *Ferroelectric and Antiferroelectric Liquid Crystals* (Wiley-VCH, Weinheim, 1999), p. 170.
[6] A. Kocot, J. K. Vij, and T. S. Perova, in Advances in Liquid Crystals, edited by J. K. Vij [special issue of Adv. Chem. Phys. **113**, 203 (2000)].
[7] H. Toriumi, H. Sugisawa, and H. Watanabe, Jpn. J. Appl. Phys., Part 2 **27**, L935 (1988).
[8] V. G. Gregoriou, J. L. Chao, H. Toriumi, and R. A. Palmer, Chem. Phys. Lett. **179**, 491 (1991).
[9] T. Urano and H. Hamaguchi, Chem. Phys. Lett. **195**, 287 (1992).
[10] T. Takano, T. Yokoyama, and H. Toriumi, Appl. Spectrosc. **47**, 1354 (1993).
[11] H. Sasaki, M. Ishibashi, A. Tanaka, N. Shibuya, and R. Hasegawa, Appl. Spectrosc. **47**, 1390 (1993).
[12] S. V. Shilov, S. Okretic, and H. W. Siesler, Vib. Spectrosc. **9**,

57 (1995).
[13] K. Masutani, H. Sugisawa, A. Yokota, Y. Furukawa, and M. Tasumi, Appl. Spectrosc. **46**, 560 (1992).
[14] K. Masutani, A. Yokota, Y. Furukawa, M. Tasumi, and A. Yoshizawa, Appl. Spectrosc. **47**, 1370 (1993).
[15] M. A. Czarnecki, N. Katayama, Y. Ozaki, M. Satoh, K. Yoshio, T. Watanabe, and T. Yanagi, Appl. Spectrosc. **47**, 1382 (1993).
[16] T. Urano and H. Hamaguchi, Appl. Spectrosc. **47**, 2108 (1993).
[17] M. A. Czarnecki, S. Okretic, and H. W. Siesler, J. Phys. Chem. B **101**, 374 (1997).
[18] M. A. Czarnecki, N. Katayama, M. Satoh, T. Watanabe, and Y. Ozaki, J. Phys. Chem. **99**, 14 (1995).
[19] N. Katayama, T. Sato, Y. Ozaki, K. Murashiro, M. Kikuchi, S. Saito, D. Demus, T. Yuzawa, and H. Hamaguchi, Appl. Spectrosc. **49**, 977 (1995).
[20] K. H. Kim, K. Miyachi, K. Ishikawa, H. Takezoe, and A. Fukuda, Jpn. J. Appl. Phys. Part 1 **33**, 5850 (1994).
[21] S. V. Shilov, S. Okretic, H. W. Siesler, R. Zentel, and T. Oege, Macromol. Rapid Commun. **16**, 125 (1995).
[22] N. Katayama, M. A. Czarnecki, Y. Ozaki, K. Murashiro, M. Kikuchi, S. Saito, and D. Demus, Ferroelectrics **147**, 441 (1993).
[23] F. Hide, N. A. Clark, K. Nito, A. Yasuda, and D. M. Walba, Phys. Rev. Lett. **75**, 2344 (1995).
[24] S. V. Shilov, S. Okretic, H. W. Siesler, and M. A. Czarnecki, Appl. Spectrosc. Rev. **31**, 82 (1996).
[25] K. H. Kim, K. Ishikawa, H. Takezoe, and A. Fukuda, Phys. Rev. E **51**, 2166 (1995).
[26] B. Jin, Z. Ling, Y. Takanishi, K. Ishikawa, H. Takezoe, A. Fukuda, M. Kakimoto, and T. Kitazume, Phys. Rev. E **53**, R4295 (1996).
[27] S. V. Shilov, H. Skupin, F. Kremer, T. Wittig, and R. Zentel, Phys. Rev. Lett. **79**, 1668 (1997).
[28] A. L. Verma, B. Zhao, S. M. Jiang, J. C. Shen, and Y. Ozaki, Phys. Rev. E **56**, 3053 (1997).
[29] A. L. Verma, B. Zhao, H. Terauchi, and Y. Ozaki, Phys. Rev. E **59**, 1868 (1999).
[30] Y. Nagasaki, T. Yoshihara, and Y. Ozaki, J. Phys. Chem. B **104**, 2846 (2000).
[31] Y. Nagasaki, K. Masutani, T. Yoshihara and Y. Ozaki, J. Phys. Chem. B **104**, 7881 (2000).
[32] W. G. Jang, C. S. Park, and N. A. Clark, Phys. Rev. E **62**, 5154 (2000).
[33] A. L. Verma, B. Zhao, A. Bhattacharjee, and Y. Ozaki, Phys. Rev. E **63**, 051704-1 (2001).
[34] A. Kocot, R. Wzralik, B. Orgasingka, T. Perova, J. K. Vij, and H. T. Nguyen, Phys. Rev. E **59**, 551 (1999).
[35] J. G. Zhao, T. Yoshihara, H. W. Siesler, and Y. Ozaki, Phys. Rev. E **64**, 031704-1 (2001).
[36] T. Yoshihara, Y. Kiyota, H. Shiroto, T. Makino, A. Mochizuki, and H. Inoue, in Proceedings of the 17th International Liquid Crystal Conference, Strasbourg, France, edited by A. Skoulios and D. Guillon [Mol. Cryst. Liq. Cryst. **331**, 217 (1999)].
[37] K. Masutani, K. Numahata, K. Nishimura, S. Ochiai, Y. Nagasaki, N. Katayama, and Y. Ozaki, Appl. Spectrosc. **53**, 588 (1999).
[38] Y. Nagasaki, K. Masutani, N. Katayama, T. Yoshihara, K. Numahata, K. Nishimura, S. Ochiai, and Y. Ozaki, Int. J. Vibr. Spectrosc. **3**, 5 (1999).
[39] I. C. Khoo, *Liquid Crystals: Physical Properties and Nonlinear Optical Phenomena* (Wiley, New York, 1995), p. 89.